Elimination of Limit Cycles and Overflow Oscillations in Time-Varying Lattice and Ladder Digital Filters

Julius O. Smith*

Center for Computer Research in Music and Acoustics (CCRMA)
Department of Music, Stanford University
Stanford, California 94305

Abstract

A construction is presented which shows that limit cycles and overflow oscillations can be eliminated in all prevalent forms of lattice and ladder digital filter structures, whether or not they are time varying, and whether or not the input signal is zero. In particular, the computationally efficient one-multiply lattice section can be made free of limit cycles and overflow oscillations in the time-varying, nonzero-input case. These results derive from a simplified formulation of digital filters in terms of cascade transmission-line segments.

Another byproduct of the formulation is a new normalized ladder filter (NLF) structure which has only three multiplies per section instead of four. The new NLF is, in principle, a transformer-coupled one-multiply section.

* Work supported in part by the System Development Foundation and (at Systems Control Technology, Palo Alto CA) the Rome Air Development Center under contract no. F30602-84-C-0016.

1. Introduction

Nonlinear effects of numerical roundoff error and overflow have plagued many applications of digital filters, including, for example, signal acquisition and conditioning systems. Artifacts can be particularly severe in the case of recursive filters. For example, overflow can cause a "chain reaction" of overflows due to the presence of feedback (an *overflow oscillation*), and roundoff error can result in a persistent, non-decaying "buzz" or "whistle" which lasts forever after the input signal ceases (a *limit cycle*).

Limit cycles and overflow oscillations can be suppressed by ensuring that the effects of overflow and roundoff error do not increase "signal power" relative to that of the ideal (infinite-precision) signal. Defining signal power and energy density on the level of individual signal samples is possible by following closely the basic physics of waves [2] or classical network theory [1].

The key point of this paper is that when digital filters are implemented in the form of classical cascade transmission line networks, a one-to-one correspondence can be found between each signal sample within the filter and a physical voltage or current level in an ideal transmission-line. In this context, it is quite clear how to define signal power for each delay register and for each sampling instant everywhere within the filter network. From there, ensuring "passive" computations is quite simple, even under arbitrary time-varying conditions. The only remaining task is then to show that all lattice and ladder filter structures can be obtained from the cascade transmission-line structure using network transformations which preserve exactly the signal power associated with each sample in spite of roundoff error and possible overflow.

The essential argument in eliminating limit cycles and overflow oscillations is as follows. Once finite-precision computations are adjusted to avoid increasing signal power on roundoff or overflow, the signal power in the digital filter becomes *bounded above* by the signal power in the corresponding infinite-precision filter. In this way, the infinite-precision signal power at each internal node serves as a

Lyapunov function for each internal node of the finite-precision filter. This means that the signal power at each delay element for each sampling instant within the finite-precision filter can never be larger than in the ideal case. Consequently, we can interpret all numerical artifacts as attenuating distortion of the original signal—no signal can persist beyond the ideal output as is characteristic of limit cycles and overflow oscillations.

2. Background

One of the earliest treatments connecting the scattering formulation of classical network theory to digital filter theory was carried out by Fettweis [3,4,5,7]. He has used the term "wave digital filters" (WDF) for the filter structures obtained by carrying classical continuous-time "wave variables" associated with networks of capacitors, inductors, and resistors, into the discrete-time domain. Wave variables are typically defined as $x = v + Ri$ and $y = v - Ri$, where v and i denote the voltage and current at a terminal of an N-port network, and R is an arbitrary "reference impedance." In wave digital filter theory, the analog frequency variable is mapped to the digital frequency variable via the bilinear conformal mapping $s = (z-1)/(z+1)$. In this formulation, it is not obvious to what extent the well-known physical properties of the analog prototype filters have been carried over to the discrete-time domain, particularly in the time-carying case. However, Fettweis [5] and Meerkötter [9] have made use of "pseudo-passivity" conditions to develop digital filter structures which are guaranteed to be free of limit cycles and overflow oscillations in the time-invariant, zero-input case.

The well-known ladder and lattice filters used in speech modeling and spectrum estimation [8,10,11,13,16] and the more recent "orthogonal filters" deriving from state-space and Nerode projection techniques [14,15] can also be derived from classical scattering theory. Gray [10,13] has used a type of pseudo-passivity (Lyapunov) theory to demonstrate that the major existing ladder and lattice filter structures can be made free of limit cycles and overflow oscillations, in the time-invariant,

zero-input case, by using extended internal precision within each section and using magnitude truncation for the final outgoing pair of samples [6,13]. Moreover, Gray proved [13] that the normalized ladder filter (NLF) is free of limit cycles and overflow oscillations even in the *time-varying,* zero-input case.

In this paper, we extend the results of Fettweis, Meerkötter, Gray, and others to include all of the well-known ladder and lattice filter structures in the time-varying, nonzero-input case. Analogous results have been obtained also for generalized multi-input, multi-output lattice filter structures [17]. These results are immediate from a reformulation of the basic theory at the most fundamental level. The formulation is closely related to the classical scattering theory, except that (1) the wave variables are pure voltage or current on a transmission-line—not linear combinations of the two, and (2) scattering points are formed by coupling transmission-line sections rather than "adapting" two RLC networks of differing "reference impedance" together. The resulting filter structure is termed a *waveguide filter* (WGF), and the WGF can be transformed into common ladder and lattice structures by network equivalence operations. The advantage of working with the WGF structure is that it corresponds *exactly* to a physical interconnection of uniform transmission-lines. This enables immediate determination of true passivity, as opposed to "pseudo-passivity."

3. The Waveguide Filter Structure

A single waveguide section between two partial sections is shown in Fig. 1. The sections are numbered 1 through 3 from left to right. For definiteness, suppose that the waveguide is *acoustic,* and that the signal variables are pressure and volume velocity. A more elaborate treatment of the acoustic tube can be found in [11]. Each waveguide section is characterized by a real, positive *characteristic impedance* $Z_i(t)$ which is allowed to vary with time, but which is constant across a waveguide section at any given instant. In the ith section, there are two pressure traveling waves: P_i^+ traveling to the right at speed c and P_i^- traveling to the left at speed c.

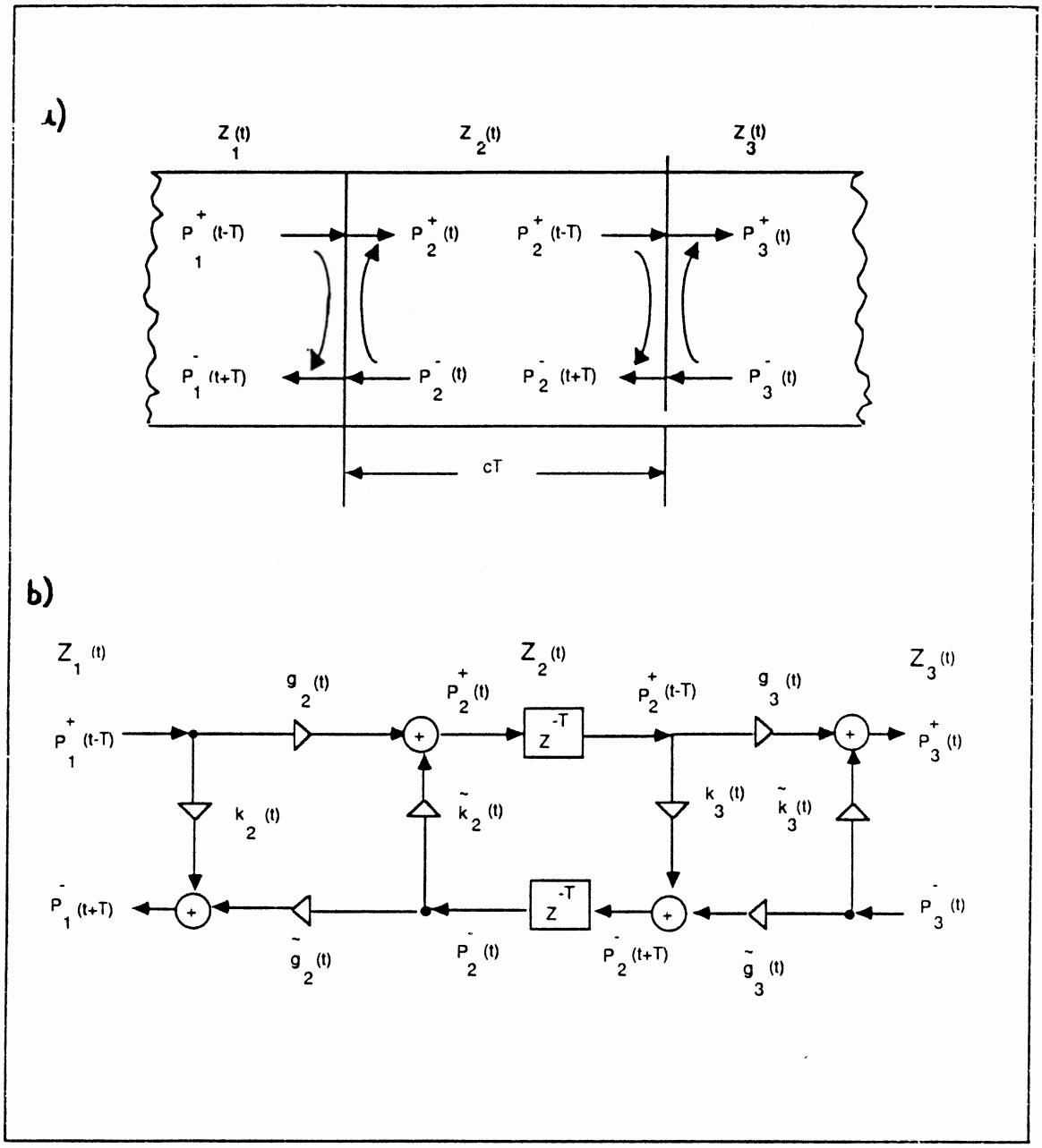

Figure 1. A waveguide section between two partial sections.

a) Physical picture indicating traveling waves in a continuous medium whose characteristic impedance changes from Z_1 to Z_2 to Z_3.

b) Digital simulation diagram for the same situation. The section traversal delay is denoted as z^{-T}. The behavior at an impedance discontinuity is characterized by forward and reverse transmission $(\tau_i, \tilde{\tau}_i)$ and reflection $(k_i, \tilde{k}_i)$ coefficients.

For minimization of dynamic range requirements, we may sometimes choose instead left- and right-going *velocity* waves, U_i^-, U_i^+, respectively, as the signal variables.

The fundamental equations relating the traveling waves and characteristic impedance in the ith section are

$$\begin{aligned} P_i^+ &= Z_i U_i^+ \\ P_i^- &= -Z_i U_i^- \end{aligned} \tag{1}$$

These will be referred to below as *Ohm's law* for unidirectional traveling waves. More precisely, $P_i^+(x,t) = Z_i(x,t)U_i^+(x,t)$ and $P_i^-(x,t) = -Z_i(x,t)U_i^-(x,t)$, where x is horizontal position along the waveguide axis and t is time. However, since (1) holds at any fixed point in space and time within each section, the arguments '(x,t)' can be dropped in the general case for simplicity of notation.

If the characteristic impedance Z_i is constant, the shape of a traveling wave is not altered as it propagates from one end of a section to the other. In this case we need only consider P_i^+ and P_i^- at one end of each section as a function of time. As shown in Fig. 1, we define $P_i^{\pm}(t)$ as the pressure at the *extreme left* of section i. Therefore, at the extreme right of section i, we have the traveling waves $P_i^+(t-T)$ and $P_i^-(t+T)$, where T is the travel time from one end of a section to the other.

When the characteristic impedances are time-varying, a number of possibilities exist which satisfy Ohm's law (1). For the moment, we will assume the traveling waves at the extreme right of section i are still given by $P_i^+(t-T)$ and $P_i^-(t+T)$. This definition, however, implies the velocity varies inversely with the characteristic impedance. As a result, signal energy is "pumped" into the waveguide by a changing characteristic impedance. The appendix describes normalization strategies which holds signal power fixed in the time-varying case.

The physical instantaneous pressure and velocity in section i are obtained by

summing the left- and right-going traveling wave components:

$$\begin{aligned} P_i &= P_i^+ + P_i^- \\ U_i &= U_i^+ + U_i^- \end{aligned} \tag{2}$$

Again this relationship is instantaneous with respect to space and time. Let $P_i(x,t)$ denote the instantaneous pressure at position x and time t in section i, where x is measured from the extreme left of section i (i.e., $0 \leq x \leq cT$). Then we have, for example, $P_i(0,t) \triangleq P_i^+(t) + P_i^-(t)$ and $P_i(cT,t) \triangleq P_i^+(t-T) + P_i^-(t+T)$ at the boundaries of section i.

Conservation of energy and mass dictate that the instantaneous pressure and velocity must be continuous across an impedance discontinuity, i.e.,

$$\begin{aligned} P_{i-1}(cT,t) &= P_i(0,t) \\ U_{i-1}(cT,t) &= U_i(0,t) \end{aligned} \tag{3}$$

Equations (1,2,3) imply the following *scattering equations:*

$$\begin{aligned} P_i^+(t) &= [1+k_i(t)]P_{i-1}^+(t-T) - k_i(t)P_i^-(t) \\ P_{i-1}^-(t+T) &= k_i(t)P_{i-1}^+(t-T) + [1-k_i(t)]P_i^-(t) \end{aligned} \tag{4}$$

where

$$k_i(t) \triangleq \frac{Z_i(t) - Z_{i-1}(t)}{Z_i(t) + Z_{i-1}(t)} \tag{5}$$

is called the ith *reflection coefficient.*

The scattering equations are illustrated in Fig. 2.* This scattering configuration is used in the *Kelly-Lochbaum* acoustic tube model [11].

---

* In the case of traveling velocity waves, the forward and reverse transmission coefficients are interchanged. However, we cannot mix pressure and velocity sections in the time-varying case unless we interject a "transformer" when changing from pressure to velocity as discussed in the appendix.

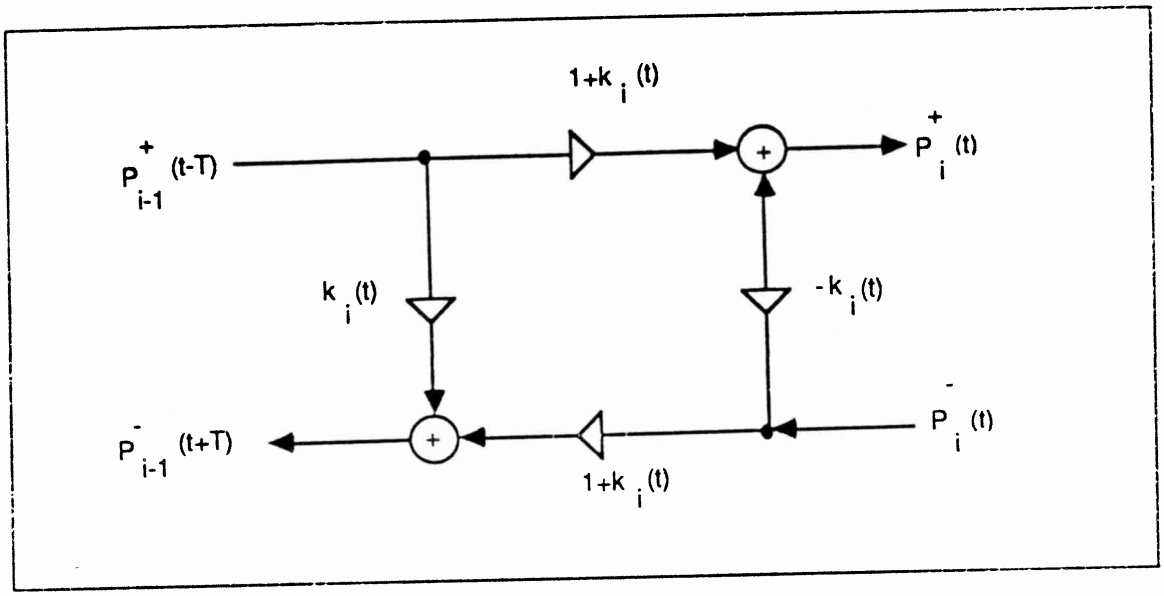

Figure 2. The Kelly-Lochbaum scattering junction.

By factoring out $k_i(t)$ in each equation of (4), we can write

$$\begin{aligned} P_i^+(t) &= P_{i-1}^+(t-T) + P_\Delta(t) \\ P_{i-1}^-(t+T) &= P_i^-(t) + P_\Delta(t) \end{aligned} \tag{6}$$

where

$$P_\Delta(t) = k_i(t)\left[P_{i-1}^+(t-T) - P_i^-(t)\right] \tag{7}$$

Thus, only one multiplication is actually necessary to compute the reflected waves from the incoming waves in the Kelly-Lochbaum junction. This computation is shown schematically in Fig. 3, and it is known as the *one-multiply* scattering junction [11]. In fixed-point implementations, the only source of error would typically be in single multiplication within the computation of P_Δ.

Another one-multiply form is obtained by organizing (4) as

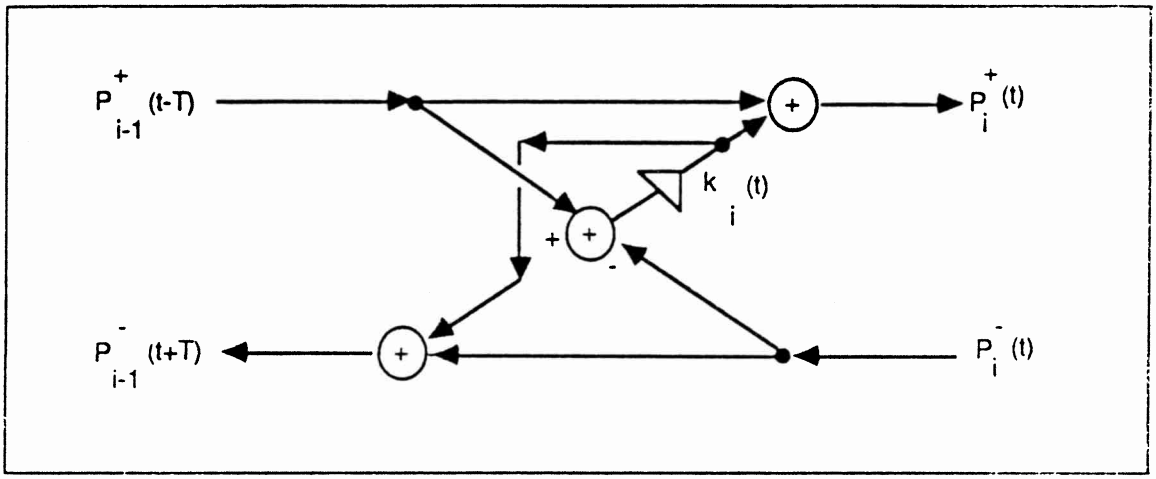

Figure 3. The one-multiply scattering boundary.

$$\begin{aligned} P_i^+(t) &= P_i^-(t) + \alpha_i(t)\tilde{P}_\Delta(t) \\ P_{i-1}^-(t+T) &= P_i^+(t) - \tilde{P}_\Delta(t) \end{aligned} \tag{8}$$

where

$$\begin{aligned} \alpha_i(t) &\triangleq 1 + k_i(t) \\ \tilde{P}_\Delta(t) &\triangleq P_{i-1}^+(t-T) - P_i^-(t) \end{aligned} \tag{9}$$

As in the previous case, only one multiplication and three additions are required per junction.

It is easy to show using the formulas of the next section that for junction passivity, the single section parameter k_i of (6) must lie between -1 and 1, while in (8), the parameter α_i must lie between 0 and 2.

4. Signal Power

The *instantaneous power* in a waveguide section containing instantaneous pressure $P_i(x,t)$ and velocity $U_i(x,t)$ is defined as the product of pressure and velocity:

$$I_i(x,t) = P_i(x,t)U_i(x,t) \tag{10}$$

An analogous definition (using the para-Hermitian conjugate of P_i) works out very well for the generalized case in which $P_i^{\pm}$ and $U_i^{\pm}$ are q by m matrices of meromorphic transfer functions [17].

The *right-going* and *left-going* power at the extreme left of the ith waveguide section are defined, respectively, by

$$\begin{aligned} I_i^+(t) &= P_i^+(t)U_i^+(t) = \frac{[P_i^+(t)]^2}{Z_i(t)} \\ I_i^-(t) &= P_i^-(t)U_i^-(t) = -\frac{[P_i^-(t)]^2}{Z_i(t)} \end{aligned} \tag{11}$$

From (10), we have $I_i(0,t) = I_i^+(t) + I_i^-(t)$ for the net power flow into the ith waveguide section from the left. The power equation completes the basic picture of interconnected waveguide sections.

5. Junction Passivity

A junction is passive if the power flowing away from it does not exceed the power flowing into it. Referring to equations (4) and (11), the total power flowing away from the ith junction is bounded by the incoming power if

$$\frac{[P_i^+(t)]^2}{Z_i(t)} + \frac{[P_{i-1}^-(t+T)]^2}{Z_{i-1}(t)} \leq \frac{[P_{i-1}^+(t-T)]^2}{Z_{i-1}(t)} + \frac{[P_i^-(t)]^2}{Z_i(t)} \tag{12}$$

which is true if and only if $I_{i-1}(cT,t) \geq I_i(0,t)$. Let $\hat{P}$ denote the finite-precision version of P. Then a *sufficient* condition for junction passivity is

$$\begin{aligned} \left|\hat{P}_i^+(t)\right| &\leq \left|P_i^+(t)\right| \\ \left|\hat{P}_{i-1}^-(t+T)\right| &\leq \left|P_{i-1}^-(t+T)\right| \end{aligned} \tag{13}$$

Thus, if the junction computations do not increase either of the output pressure amplitudes, no signal power is created. An analogous conclusion is reached for velocity scattering junctions.

6. Passive Arithmetic

In a finite-precision implementation, only the junction output signals $\hat{P}_i^+(t)$ and $\hat{P}_{i-1}^-(t+T)$ need to be examined as possible sources of increased signal power. Quantized reflection coefficients $\hat{k}_i(t)$ (between 0 and 1) can be regarded as error-free (insofar as passivity is concerned) because to each sequence of quantized reflection coefficients, $\hat{k}_i(t), i = 1,\ldots,M$, there corresponds a sequence of exact characteristic impedances $\hat{Z}_i(t) = \hat{Z}_{i-1}(t)[1+\hat{k}_i(t)]/[1-\hat{k}_i(t)], i = 1,\ldots,M+1$, where $\hat{Z}_0$ is arbitrary and $\hat{Z}_{M+1}$ is infinity. The quantized input signals $\hat{P}_{i-1}^+(t-T)$ and $\hat{P}_i^-(t)$ are simply delayed outputs from adjoining junctions, and the intervening delay lines introduce no further quantization.

In view of the previous paragraph and equation (13), a general means of obtaining passive junctions is to compute exact results internally using extended precision, and apply saturation and magnitude truncation to the final outgoing waves. Let

$$\begin{aligned} n &\triangleq \text{Number of bits per signal sample} \\ m &\triangleq \text{Number of bits per reflection-coefficient} \end{aligned} \tag{14}$$

We assume fractional two's complement arithmetic is used, although analogous results exist for other number systems. Both the signal variables $P_i^{\pm}$ and the

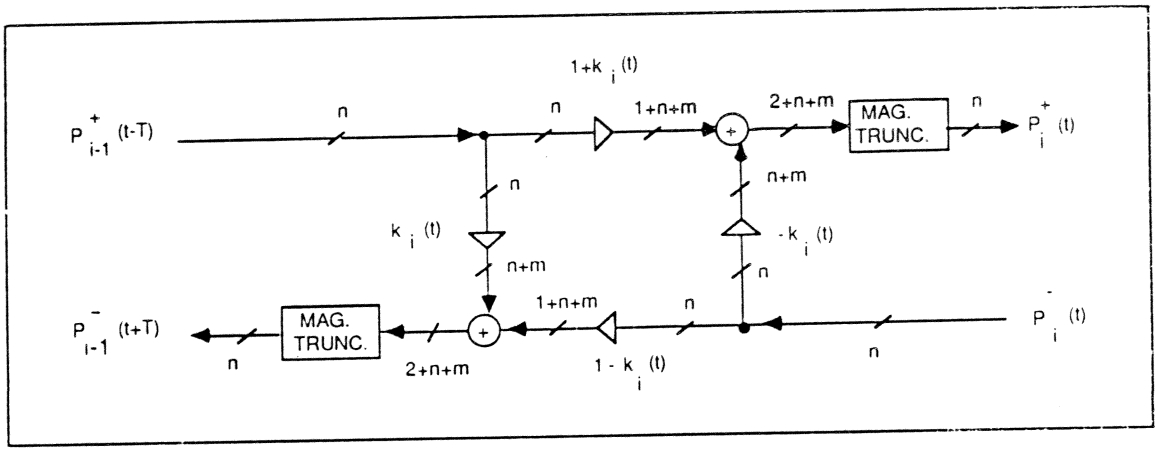

Figure 4. Bit allocations in the passive, finite-precision, Kelly-Lochbaum junction.

reflection coefficients k_i are assumed to lie between -1 and 1 so that the binary point is at the far left in every case.

7. The Passive Kelly-Lochbaum Junction

Figure 4 shows the number of bits needed to implement a passive Kelly-Lochbaum junction. The forward and reverse transmission coefficients each require $m+1$ bits in order that $1 \pm \hat{k}_i(t)$ be represented exactly relative to $\hat{k}_i(t)$. When an n-bit value is multiplied by an m-bit value, the complete product contains $n+m$ bits, in general. Similarly, an n-bit value added to an m-bit value requires $1+\max\{n,m\}$ bits to represent exactly all possible results.

The error-free junction outputs occupy $2+n+m$ bits. The 2 most-significant bits (MSB's) and the m least-significant bits (LSB's) must be discarded. When the 3 MSB's are not equal, overflow has occurred. The 2 MSB's can simply be discarded (resulting in "wrap-around" on overflow), or they can be used replace the output value by the maximum-magnitude number in n-bit two's complement having the correct sign ("saturation" on overflow). The 3 MSB's determine the appropriate

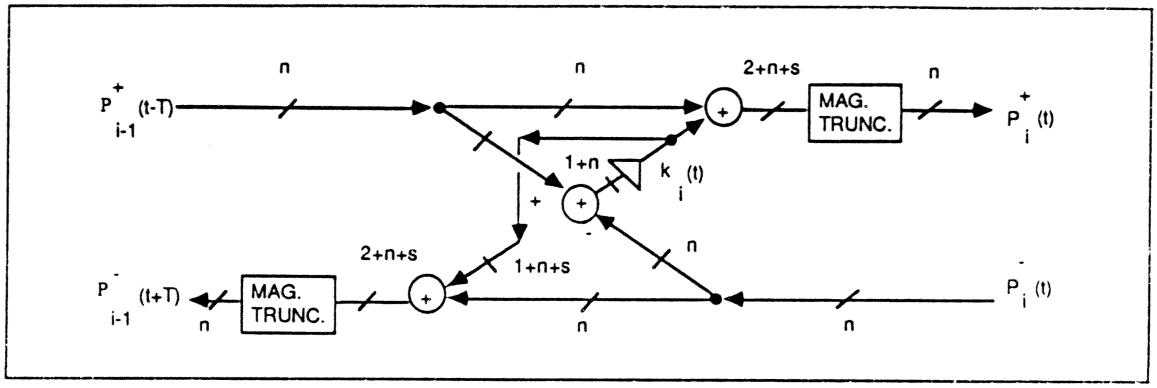

Figure 5. Bit allocations in the passive, finite-precision, one-multiply junction.

action to take in a saturating adder. With either overflow-handling strategy, the signal amplitude is reduced upon overflow. Consequently, by (13), signal power is always decreased by output adder overflow, even in the otherwise disastrous case of two's complement "wrap-around."

The magnitude truncation function discards the low-order (least significant) m bits of the result if it is positive. The low-order m bits are also discarded if they are all zero. If the extended-precision result is negative and any of the m low-order bits is nonzero, then the smallest positive number (2^{-n+1}) is added to the value obtained by discarding the low-order m bits. Thus, the number is always *truncated toward zero.*

A simpler magnitude truncation scheme which loses the LSB with probability 2^{-m} is to simply discard the low-order m bits in all cases, and always add 2^{-n+1} to the n-bit result if it is negative.

8. The Passive One-Multiply Junction

Figure 5 shows the number of bits needed to implement a passive one-multiply junction. The adder before the reflection coefficient increases the signal width by

one bit, and the reflection coefficient itself adds m bits, for a total of $1 + n + m$ bits going into each of the two final adders. The final output signal again occupies $2 + n + m$ bits. Output overflow considerations are exactly the same as in the Kelly-Lochbaum junction. However, the magnitude truncation is less expensive in the present case. Notice in Fig. 5 that *every adder has at least one operand consisting of only n bits.* Consequently, the low-order m bits at the input to the two output adders will be summed with zeros and passed through unchanged. Hence, the adders need not accept the low-order m bits. The logical OR of all of the m LSB's of the multiplier output (denoted s in Fig. 5) can be fed directly to the magnitude truncation unit, without increasing the adder complexity at all. In the simplified magnitude truncation scheme, the low-order m bits from the multiplier can be ignored completely. With some multiplier chips, the low-order product must be extracted on a separate output tri-state enable; in this situation, the simplified magnitude truncation scheme may double throughput.

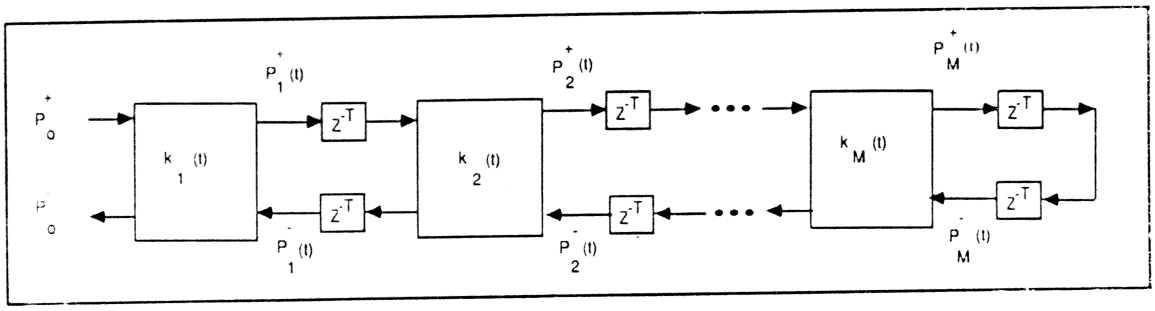

Figure 6. Waveguide digital filter structure.

9. Reduction to Standard Forms

The basic WGF we have been considering is shown in Fig. 6. Each box enclosing the symbol $k_i(t)$ denotes a scattering junction characterized by $k_i(t)$. While we have mentioned only the Kelly-Lochbaum and one-multiply junction, any type of lossless junction will do. In particular, the two-multiply lattice and normalized ladder scattering junctions [11] can appear in these boxes.*The WGF employs delays between each scattering junction along both the top and bottom signal paths, unlike conventional ladder and lattice filters. Reduction to the standard forms is merely a matter of pushing delays along the top rail around to the bottom rail, so that each bottom-rail delay becomes $2T$ seconds instead of T seconds. Such an operation is possible because of the termination at the right by an infinite (or zero) characteristic impedance.

In the time-varying case, pushing a delay through a multiply results in a corresponding time advance of the multiplier coefficient, as shown in Fig. 7.

---

* According to lore, when the diagram within each junction box is a *planar* graph, as in the Kelly-Lochbaum and normalized ladder junction, the resulting system is called a *ladder* filter. When the junction scattering diagrams are *nonplanar,* as in the one-multiply or two-multiply cases, the term *lattice* filter is used. However, this definition appears not to be universal.

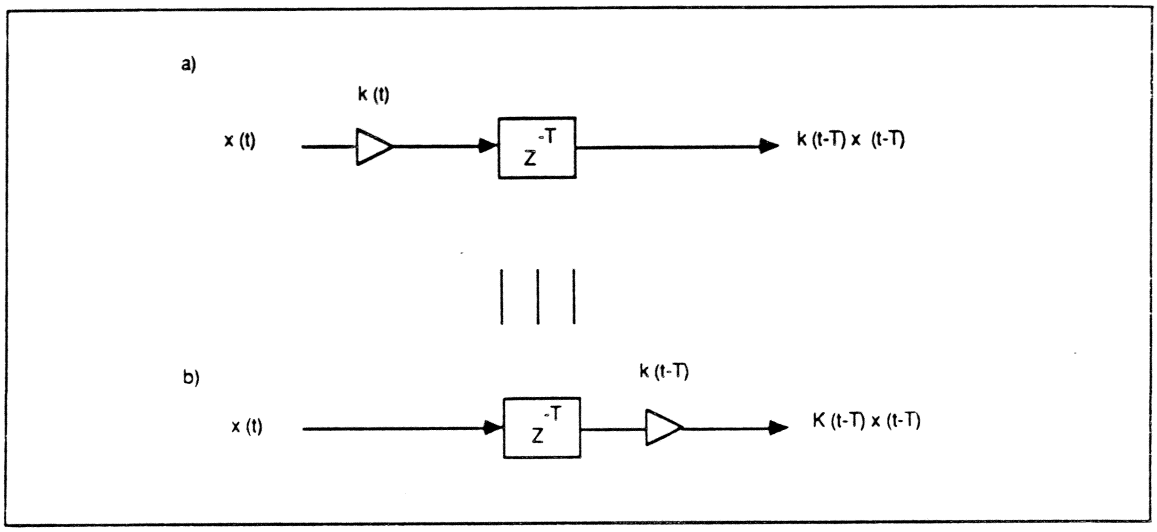

Figure 7. Commuting a delay with a multiplier coefficient in the time-varying case.

Imagine each delay element in Fig. 6 being divided into halves, and let q denote a delay of $T/2$ seconds. Then any WGF can be built from sections such as shown in Fig. 8a.

The series of transformations shown in Fig. 8 push the two input-signal delays through the junction to the two output delays. A similar sequence of moves pushes the two output delays into the two input branches. Consequently, we can replace any WGF section of the form shown in Fig. 9a by a section of the form shown in Fig. 9b or c.

By alternately choosing the structure of Fig. 9b and c, the filter structure of Fig. 10 is obtained. This structure has some advantages worth considering: (1) it consolidates delays to length $2T$ as do conventional lattice/ladder structures, (2) it does not require a termination by an infinite characteristic impedance, allowing it to be extended to networks of arbitrary topology (e.g., multiport branching, intersection, and looping), and (3) there is no long delay-free signal path along the upper rail as in conventional structures—a pipeline segment is only two sections long. This structure, termed the "half-rate waveguide filter" [17], appears to

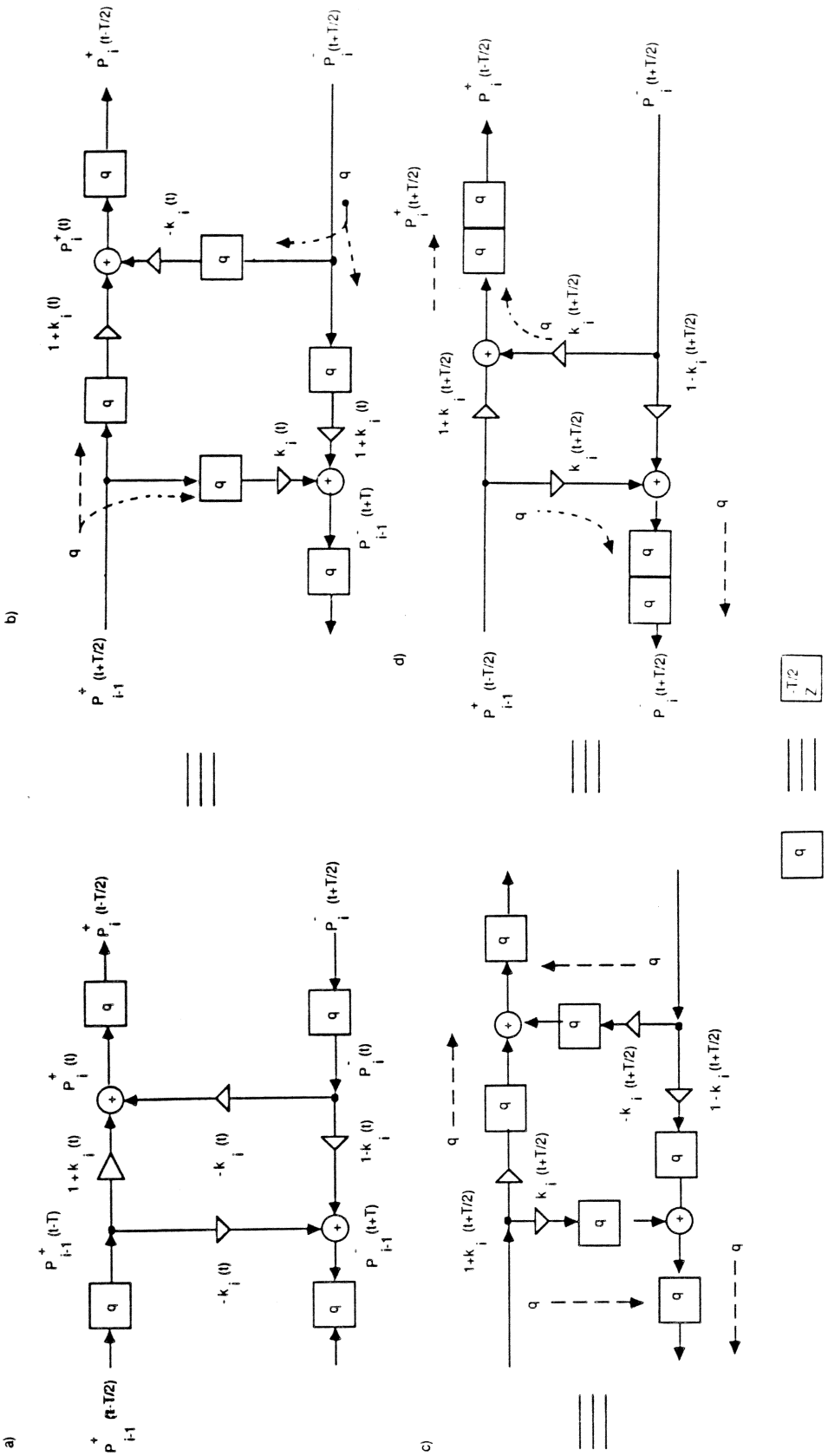

Figure 8. Consolidating delays by pushing through the junction.

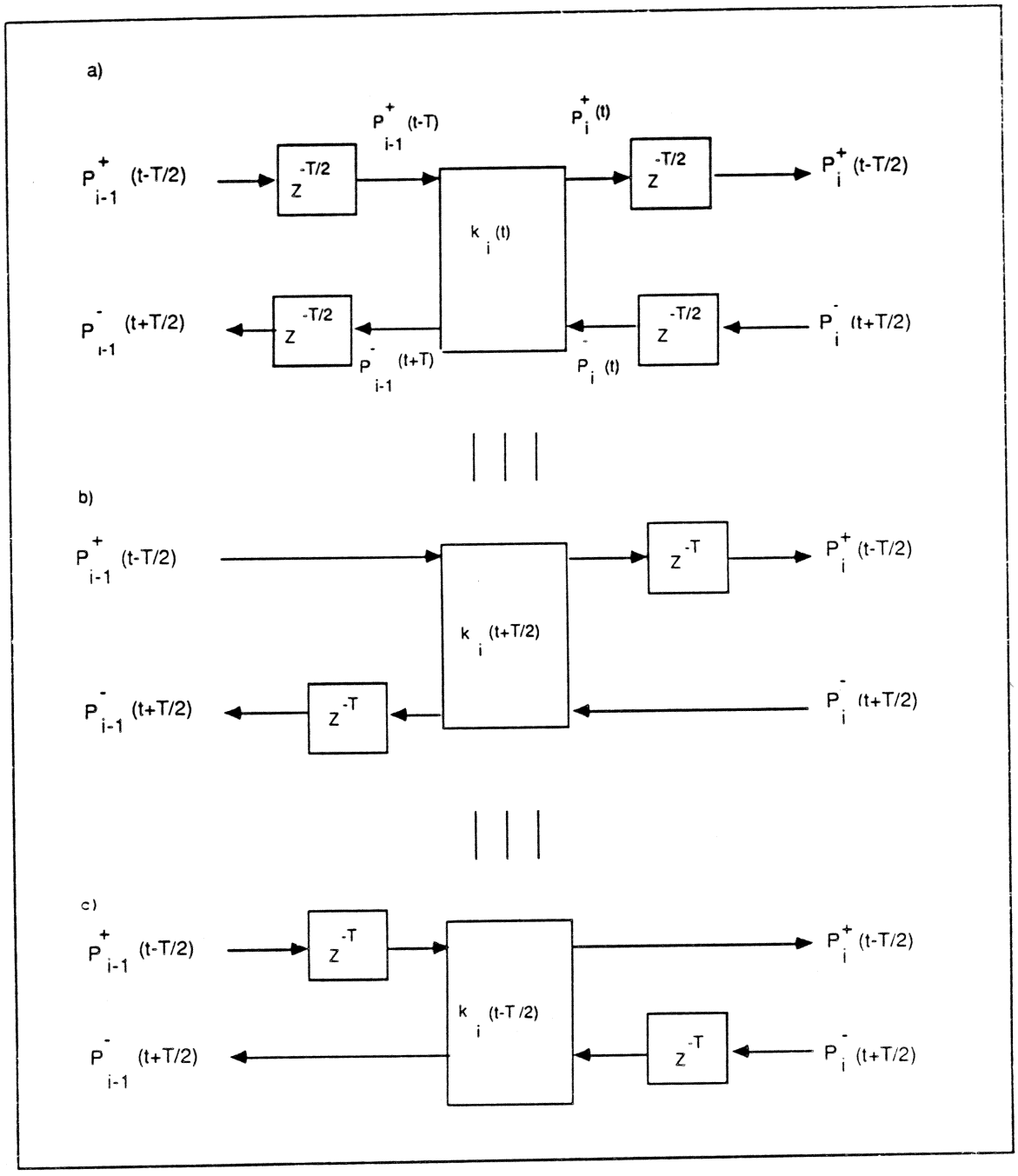

Figure 9. Equivalent waveguide filter sections.

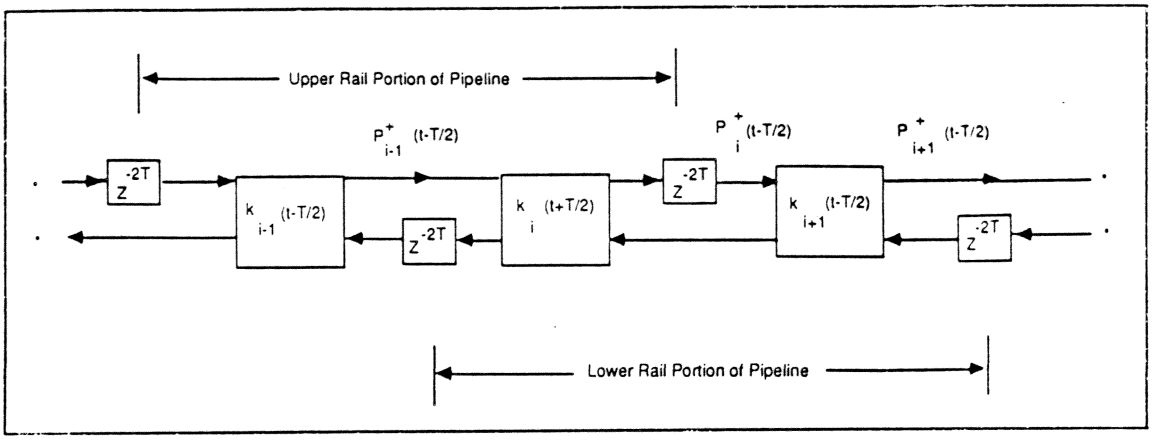

Figure 10. Pipelineable, physically extendible, consolidated-delay, waveguide filter.

have better overall characteristics than any other digital filter structure for many applications. Advantage (2) makes it especially valuable for modeling physical systems.

Finally, successive substitutions of the section of Fig. 9b and reapplication of the delay consolidation transformation lead to the structure of Fig. 11. This is the conventional ladder or lattice filter structure. The termination at the right by a total reflection is required to obtain this structure. Consequently, conventional lattice filters cannot be extended on the right in a physically meaningful way. Also, creating network topologies more complex than a simple series (or acyclic tree) of waveguide sections is not immediately possible because of the delay-free path along the top rail. For example, the output cannot be fed back to the input. Nevertheless, the conventional structure enjoys the same physical interpretation as the more general WGF structures, including the same simple passivity conditions in the time-varying, nonzero-input case.

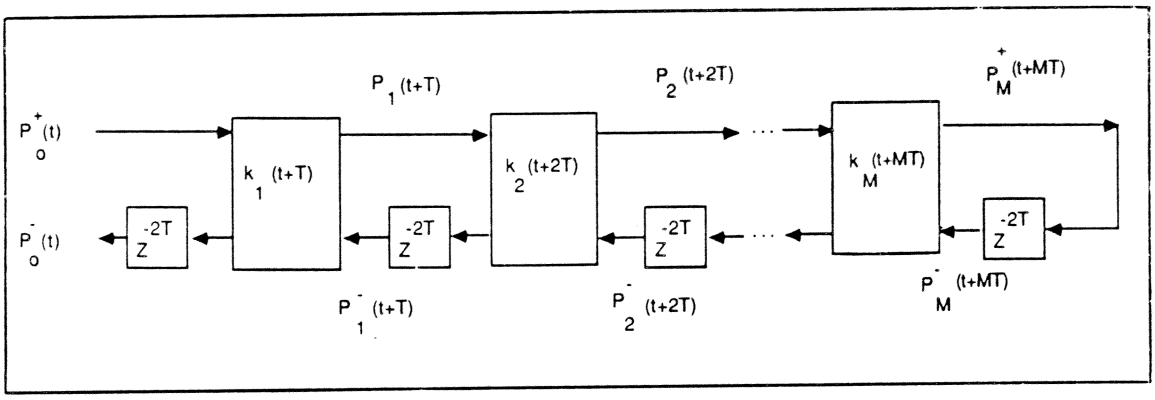

Figure 11. Conventional ladder/lattice filter structure.

10. Appendix — Power-Normalized Waveguide Filters

Above, we adopted the convention that the time variation of the characteristic impedance did not alter the traveling pressure waves $P_i^{\pm}$. In this case, the power represented by a traveling pressure wave is modulated by the changing characteristic impedance as it propagates. The actual power becomes invsersely proportional to characteristic impedance:

$$I_i(x,t) = I_i^+(x,t) + I_i^-(x,t) = \frac{[P_i^+(x,t)]^2 - [P_i^-(x,t)]^2}{Z_i(t)} \tag{15}$$

This power modulation causes no difficulties in the Lyapunov theory because it occurs identically in both the finite-precision and infinite-precision filters. However, in some applications (e.g. [18]), it may be desirable to compensate for the power modulation so that changes in the characteristic impedances of the waveguides do not affect the power of the signals propagating within.

Consider an arbitrary point in the ith waveguide at time t and distance $x = c\tau$ measured from the left boundary, as shown in Fig. 12. The right-going pressure is $P_i^+(x,t)$ and the left-going pressure is $P_i^-(x,t)$. In the absence of scaling, the

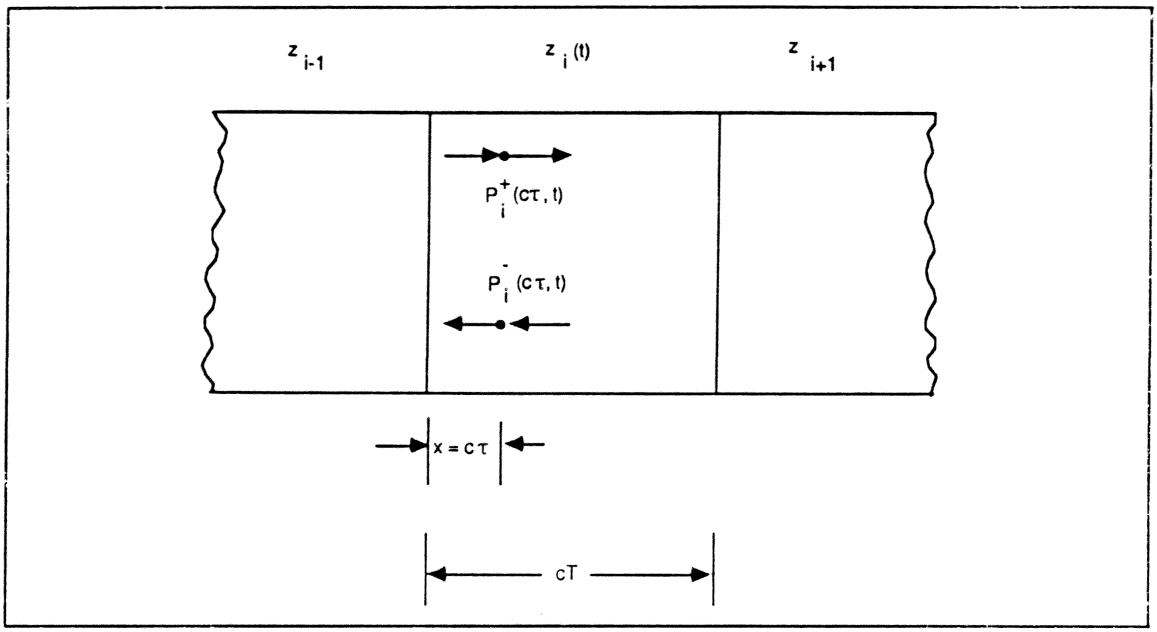

Figure 12. Traveling pressure waves at a general point within a waveguide section.

waveguide section behaves (according to our definition of the propagation medium properties) as a pressure delay line, and we have $P_i^+(x,t) = P_i^+(0,t-\tau)$ and $P_i^-(x,t) = P_i^-(0,t+\tau) = P_i^-(cT,t-T+\tau)$. The left-going and right-going components of the signal power are $[P_i^+(x,t)]^2/Z_i(t)$ and $[P_i^-(x,t)]^2/Z_i(t)$, respectively.

Below, three methods are discussed for making signal power *invariant* with respect to time-varying branch impedances.

10.1. Normalized Waveguides

Suppose we are willing to scale the traveling waves as the characteristic impedance changes in order to hold signal power fixed. We can choose any position as a reference, but perhaps it is most natural to fix the power of each wave to that which it had upon entry to the section. In this case, it is quickly verified that the

proper scaling is

$$\begin{aligned}\tilde{P}_i^+(x,t) &= \left(\frac{Z_i(t)}{Z_i(t-\tau)}\right)^{1/2} P_i^+(0,t-\tau), \qquad x = c\tau \\ \tilde{P}_i^-(x,t) &= \left(\frac{Z_i(t)}{Z_i(t-T+\tau)}\right)^{1/2} P_i^-(cT,t-T+\tau)\end{aligned} \tag{16}$$

In practice, there is no need to perform the scaling until the signal actually reaches a junction. Thus, we implement

$$\begin{aligned}\tilde{P}_i^+(cT,t) &= g_i(t)P_i^+(0,t-T) \\ \tilde{P}_i^-(0,t) &= g_i(t)P_i^-(cT,t-T)\end{aligned} \tag{17}$$

where

$$g_i(t) = \sqrt{\frac{Z_i(t)}{Z_i(t-T)}}$$

In the single-argument notation used earlier, (17) becomes

$$\begin{aligned}\tilde{P}_i^+(t-T) &= g_i(t)P_i^+(t-T) \\ \tilde{P}_i^-(t) &= g_i(t)P_i^-(t)\end{aligned} \tag{18}$$

A diagram of this normalization strategy is shown in Fig. 13. It has the property that the time-varying waveguides (as well as the junctions) conserve signal power. If the scattering junctions are implemented with one-multiply structures, then the number of multiplies per section rises to three when power is normalized. There are three additions as in the unnormalized case. In some situations (such as in the two-stage structure of Fig. 10), it may be acceptable to normalize at fewer points; the normalizing multiplies can be pushed through the scattering junctions and combined with other normalizing multiplies, much in the same way delays were pushed through the junctions to obtain standard ladder/lattice forms. In physical

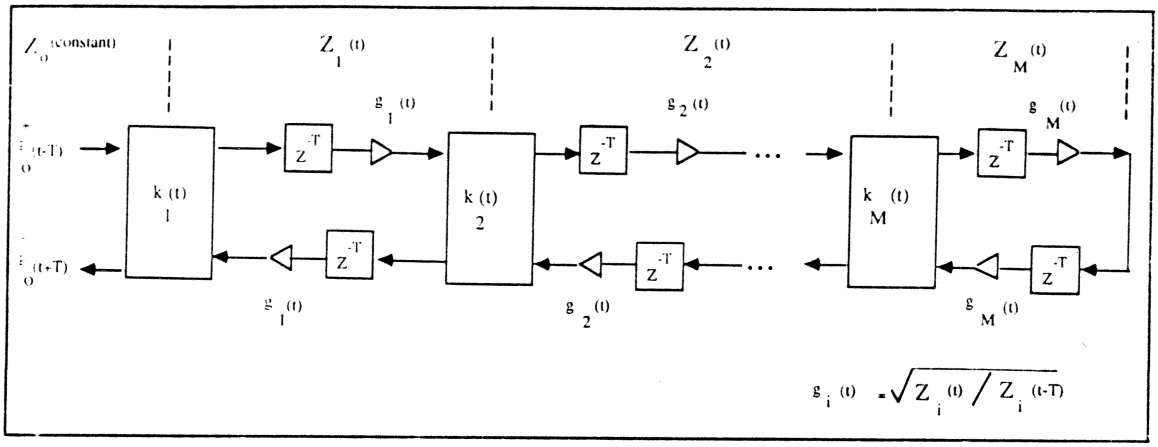

Figure 13. Normalized-waveguide digital filter structure.

modeling applications, normalization can be limited to opposite ends of a long cascade of sections with no interior output "taps."

To ensure passivity of a normalized-waveguide with finite-precision calculations, it suffices to perform magnitude truncation after multiplication by $g_i(t)$. Alternatively, extended precision can be used within the scattering junction.

10.2. Normalized Waves

Another approach to normalization is to propagate *rms-normalized waves* in the waveguide. In this case, each delay-line contains

$$\begin{aligned} \tilde{P}_i^+(x,t) &= P_i^+(x,t) \Big/ \sqrt{Z_i(t)} \\ \tilde{P}_i^-(x,t) &= P_i^-(x,t) \Big/ \sqrt{Z_i(t)} \end{aligned} \tag{19}$$

We now consider $\tilde{P}^{\pm}$ (instead of $P^{\pm}$) to be invariant with respect to the character-

istic impedance. In this case,

$$\tilde{P}_i^+(cT) = \frac{P_i^+(cT,t)}{\sqrt{Z_i(t)}} = \frac{P_i^+(0,t-T)}{\sqrt{Z_i(t-T)}} = \tilde{P}_i^+(t-T)$$

The scattering equations (4) become

$$\begin{aligned}\sqrt{Z_i(t)}\,\tilde{P}_i^+(0,t) &= [1+k_i(t)]\sqrt{Z_{i-1}(t)}\,\tilde{P}_{i-1}^+(cT,t) - k_i(t)\sqrt{Z_i(t)}\,\tilde{P}_i^-(0,t)\\ \sqrt{Z_{i-1}(t)}\,\tilde{P}_{i-1}^-(cT,t) &= k_i(t)\sqrt{Z_{i-1}(t)}\,\tilde{P}_{i-1}^+(ct,T) + [1-k_i(t)]\sqrt{Z_i(t)}\,\tilde{P}_i^-(t)\end{aligned} \tag{20}$$

or, solving for $\tilde{P}_i^{\pm}$,

$$\begin{aligned}\tilde{P}_i^+(0,t) &= [1+k_i(t)]\sqrt{\frac{Z_{i-1}(t)}{Z_i(t)}}\,\tilde{P}_{i-1}^+(cT,t) - k_i(t)\tilde{P}_i^-(0,t)\\ \tilde{P}_{i-1}^-(cT,t) &= k_i(t)\tilde{P}_{i-1}^+(ct,T) + [1-k_i(t)]\sqrt{\frac{Z_i(t)}{Z_{i-1}(t)}}\,\tilde{P}_i^-(t)\end{aligned} \tag{21}$$

But, from (5),

$$\frac{Z_{i-1}(t)}{Z_i(t)} = \frac{1-k_i(t)}{1+k_i(t)} \tag{22}$$

whence

$$[1+k_i(t)]\sqrt{\frac{Z_{i-1}(t)}{Z_i(t)}} = [1-k_i(t)]\sqrt{\frac{Z_i(t)}{Z_{i-1}(t)}} = \sqrt{1-k_i^2(t)} \tag{23}$$

The final scattering equations for normalized waves are

$$\begin{aligned}\tilde{P}_i^+(0,t) &= c_i(t)\tilde{P}_{i-1}^+(cT,t) - s_i(t)\tilde{P}_i^-(0,t)\\ \tilde{P}_{i-1}^-(cT,t) &= s_i(t)\tilde{P}_{i-1}^+(ct,T) + c_i(t)\tilde{P}_i^-(t)\end{aligned} \tag{24}$$

where

$$\begin{aligned}s_i(t) &\triangleq k_i(t)\\ c_i(t) &\triangleq \sqrt{1-k_i^2(t)}\end{aligned} \tag{25}$$

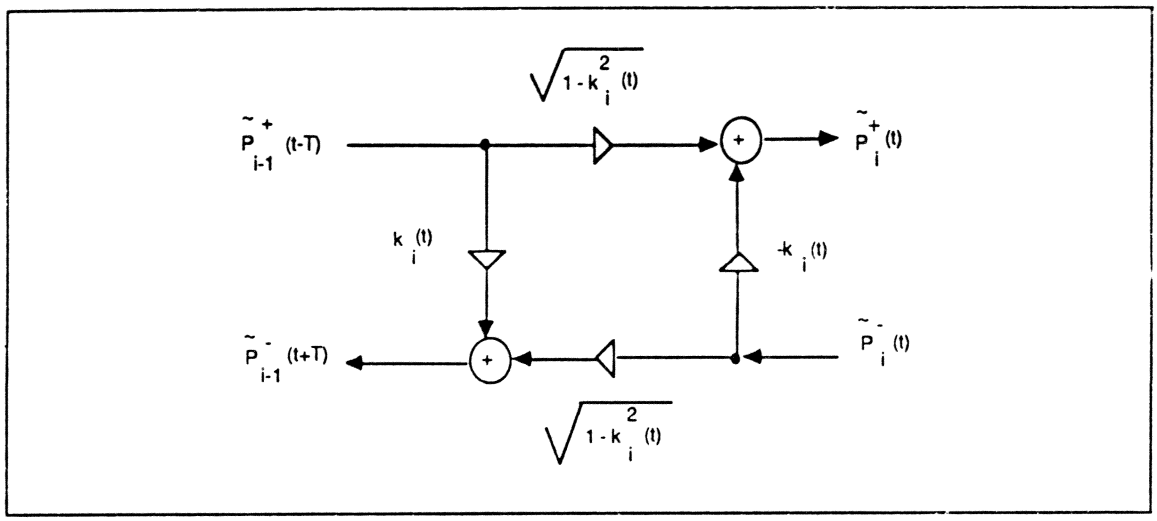

Figure 14. Wave-normalized waveguide junction.

can be viewed as the sine and cosine, respectively, of a single angle $\theta_i(t) = \sin^{-1}[k_i(t)]$ which characterizes the junction. Figure 14 illustrates the Kelly-Lochbaum junction as it applies to normalized waves. This time we cannot factor out $k_i(t)$ to obtain a one-multiply structure. The four-multiply structure of Fig. 14 is used in the *normalized ladder filter* (NLF) suggested by Gray and Markel [10,11,13].

Note that normalizing the output of the delay lines (as discussed in the previous subsection) saves one multiply relative to the NLF which propagates normalized waves. However, there are other differences to consider. In the case of normalized waves, duals are easier; i.e., changing the propagation variable from pressure to velocity or vice versa in the ith section requires no signal normalization, and the forward and reverse reflection coefficients are unchanged. Only sign-reversal is required for the reverse path. Also, in the case of normalized waves, the rms signal level is the same whether or not pressure or velocity is used. While appealing from a "balance of power" standpoint, normalizing all signals by their rms level can be a disadvantage: In the case of normalized delay-line outputs, dynamic range can minimized by choosing the smaller of pressure and velocity as the variable of propagation.

10.3. Transformer-Coupled Waveguides

Still another approach to the normalization of time-varying waveguide filters is perhaps the most convenient of all. So far, the least expensive normalization technique is the normalized-waveguide structure of Fig. 13, requiring only three multiplies per section rather than four in the normalized-wave case. Unfortunately, in the normalized-waveguide case, changing the characteristic impedance of section i results in a changing of the reflection coefficients in *both* adjacent scattering junctions. Of course, a single junction can be modulated in isolation by changing all downstream characteristic impedances by the same ratio. But this does not help if the filtering network is not a cascade chain or acyclic tree of waveguide sections. A cleaner local variation in characteristic impedance can be obtained using *transformer coupling*. A transformer joins two waveguide sections of differing characteristic impedance in such a way that signal power is preserved and no scattering occurs. It turns out that filter structures built using the transformer-coupled waveguide are *equivalent* to those using the normalized-wave junction described in the previous subsection, but one of the four multiplies can be traded for an addition.

From Ohm's law (1) and the power equation (11), we see that to bridge an impedance discontinuity with no power change and no scattering requires the relations

$$\begin{aligned} \frac{[P_i^+]^2}{Z_i(t)} &= \frac{[P_{i-1}^+]^2}{Z_{i-1}(t)} \\ \frac{[P_i^-]^2}{Z_i(t)} &= \frac{[P_{i-1}^-]^2}{Z_{i-1}(t)} \end{aligned} \tag{26}$$

Therefore, the junction equations for a *transformer* [1] can be chosen as

$$\begin{aligned} P_i^+ &= g_i(t) P_{i-1}^+ \\ P_{i-1}^- &= g_i^{-1}(t) P_i^- \end{aligned} \tag{27}$$

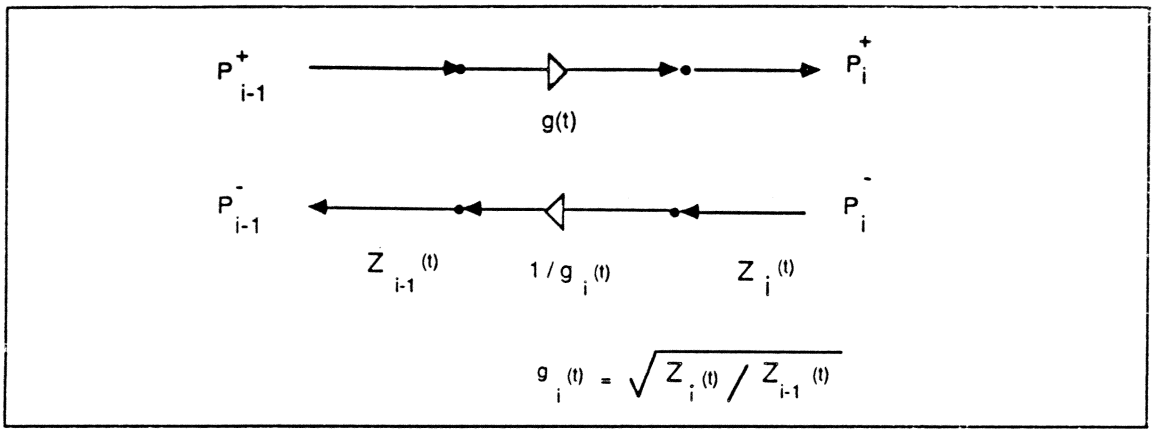

Figure 15. a) Transformer junction.

(depicted in Fig. 15) where, from (22),

$$g_i(t) \triangleq \sqrt{\frac{Z_i(t)}{Z_{i-1}(t)}} = \sqrt{\frac{1+k_i(t)}{1-k_i(t)}} \tag{28}$$

The choice of a negative square root corresponds to the *gyrator* [1]. The gyrator is equivalent to a transformer in cascade with a dualizer [17]. A dualizer is a direct implementation of Ohm's law (1) (to within a scale factor): the forward path is unchanged while the reverse path is negated. On one side of the dualizer there are pressure wave, and on the other side there are velocity waves. Ohm's law is a gyrator in cascade with a transformer whose scale factor equals the characteristic admittance.

The transformer-coupled WGF junction is shown in Fig. 16a. We can now modulate a single junction, even in arbitrary network topologies, by inserting a transformer immediately to the left or right of the junction. Conceptually, the characteristic impedance is not changed over the delay-line portion of the waveguide section; instead, it is changed to the new time-varying value just before (or after) it meets the junction. When velocity is the wave variable, the coefficients g_i and g_i^{-1} in Fig. 16a are swapped (or inverted).

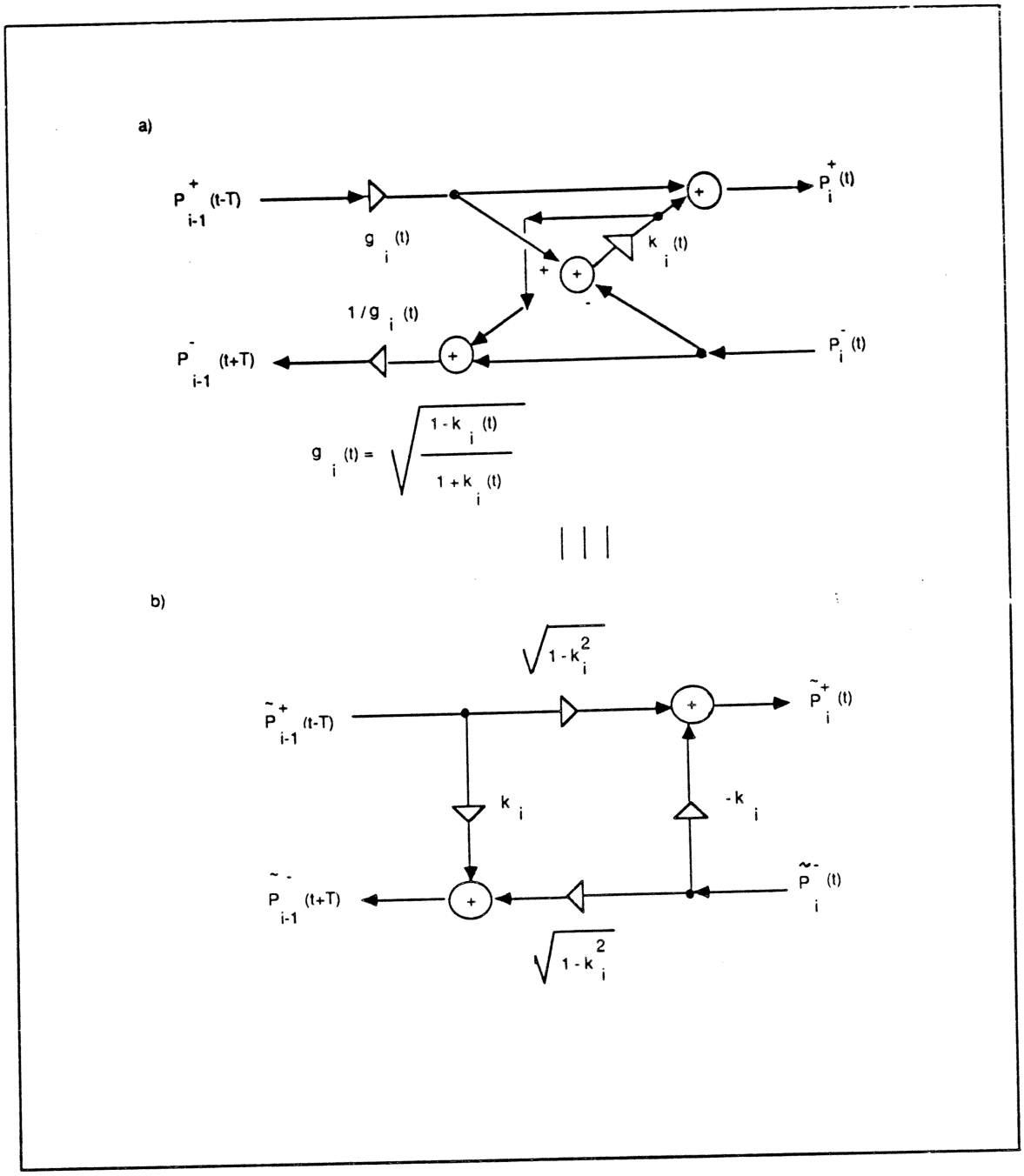

Figure 16. a) Transformer-coupled waveguide digital filter section, for transformer on left of junction. b) Normalized ladder filter section. The two are equivalent.

So, as in the normalized waveguide case, for the price of two extra multiplies per section, we can implement time-varying digital filters which do not modulate stored signal energy. Moreover, transformers enable the scattering junctions to be varied independently, without having to propagate time-varying impedance ratios throughout the waveguide network.

It is interesting to note that the transformer-coupled WGF and the wave-normalized WGF (shown in Fig. 16b) are equivalent. One simple proof is to start with a transformer and a Kelly-Lochbaum junction, move the transformer scale factors inside the junction, combine terms, and arrive at Fig. 16b. The practical importance of this equivalence is that the normalized ladder filter (NLF) can be implemented with only three multiplies and three additions instead of four multiplies and two additions.

11. Conclusions

It has been shown that limit cycles and overflow oscillations are easily eliminated in a waveguide filter (WGF) structure, which precisely simulates a sampled interconnection of ideal transmission line sections. Furthermore, the WGF can be transformed into all well-known ladder and lattice filter structures simply by pushing delays around to the bottom rail in the special case of a cascade, reflectively terminated WGF network. Therefore, aside from some time skew in the signal and filter coefficients, the samples computed in the WGF and the samples computed in other ladder/lattice filters are identical.

The WGF structure gives a precise implementation of physical wave phenomena in time-varying media. This property may be valuable in its own right for simulation purposes. It was shown how to delay or advance time-varying coefficient streams in order to obtain physically correct time-varying waveguide (or acoustic tube) simulations using standard lattice/ladder structures; also, the necessary time corrections for the traveling waves, needed to output a simulated pressure or velocity, were shown.

A reduction in the required number of multiplies per section was obtained for the well-known normalized ladder filter (NLF). While the three-multiply structure can be obtained from the four-multiply structure using network equivalence operations, its discovery is due to the simplified theoretical formulation presented in this paper.

12. References

[1] V. Belevitch, *Classical Network Theory,* Holden Day, San Francisco, CA, 1968.

[2] P. M. Morse and K. U. Ingard, *Theoretical Acoustics,* McGraw-Hill, New York, 1968.

[3] A. Fettweis, "Digital Filters Related to Classical Structures," *AEU: Archive für Elektronik und Übertragungstechnik,* vol. 25, pp. 79-89, Feb. 1971.

[4] A. Fettweis, "Some Principles of Designing Digital Filters Imitating Classical Filter Structures," *IEEE Trans. on Circ. Theory,* vol. CT-18, pp. 314-316, March 1971.

[5] A. Fettweis, "Pseudopassivity, Sensitivity, and Stability of Wave Digital Filters," *IEEE Trans. on Circ. Theory,* vol. CT-19, pp. 668-673, Nov. 1972.

[6] K. Meerkötter and W. Wegener, "A New Second-Order Digital Filter without Parasitic Oscillations," *AEU: Archive für Elektronik und Übertragungstechnik,* vol. 29, pp. 312-314, Feb. 1975.

[7] A. Fettweis and K. Meerkötter, "On Adaptors for Wave Digital Filters," *IEEE Trans. on Acoust., Speech, and Signal Proc.*, vol. ASSP-23, pp. 516-525, Dec. 1975.

[8] A. H. Gray and J. D. Markel, "Digital Lattice and Ladder Filter Synthesis," *IEEE Trans. on Audio Electroacoust.*, vol. AU-21, pp. 491-500, Dec. 1973.

[9] A. Fettweis and K. Meerkötter, "Suppression of Parasitic Oscillations in Wave Digital Filters," *IEEE Trans. Circ. and Sys.*, vol. CAS-22, No. 3, pp. 239-246, Mar. 1975.

[10] A. H. Gray and J. D. Markel, "A Normalized Digital Filter Structure," *IEEE Trans. on Acoust., Speech, and Signal Proc.*, vol. ASSP-23, pp. 268-277, June 1975.

[11] J. D. Markel and A. H. Gray, *Linear Prediction of Speech*, Springer-Verlag, New York, 1976.

[12] S. S. Lawson, "On a Generalization of the Wave Digital Filter Concept," *Int. J. Circuit Theory Appl.*, vol. 6, pp. 107-120, 1978.

[13] A. H. Gray, "Passive Cascaded Lattice Digital Filters," *IEEE Trans. Circ. and Sys.*, vol. CAS-27, No. 5, pp. 337-344, May 1980.

[14] P. DeWilde and H. Dym, "Schur Recursions, Error Formulas, and Convergence of Rational Estimators for Stationary Stochastic Estimators," *IEEE Trans. on Info. Theory*, vol. IT-27, pp. 446-461, July 1981.

[15] P. H. Delsarte, Y. V. Genin, and Y. Kamp, "On the Role of the Nevanlinna-Pick Problem in Circuit and System Theory," *Int. J. Circuit Theory Appl.*, vol. 9, no. 2, pp. 177-187, April 1981.

[16] B. Friedlander, "Lattice Filters for Adaptive Processing," *Proc. IEEE*, vol. 70, pp. 829-867, Aug. 1982.

[17] J. O. Smith, "Waveguide Digital Filters," Center for Computer Research in Music and Acoustics (CCRMA), Dept. of Music, Stanford University, March 1985.

[18] J. O. Smith, "A New Approach to Digital Reverberation using Closed Waveguide Networks," *Proc. 1985 Int. Conf. Computer Music*, Vancouver Canada, Computer Music Assoc., 1985. Music Dept. Tech. Rep. STAN-M-31, Stanford University, July 1985.